Monogamy relations of entropic non-contextual inequalities and their experimental realization

Dileep Singh,[1,*] Jaskaran Singh,[2,†] Kavita Dorai,[1,‡] and Arvind[1,3,§]

[1] *Department of Physical Sciences, Indian Institute of Science Education & Research Mohali, Sector 81 SAS Nagar, Manauli PO 140306 Punjab, India.*

[2] *Departamento de Física Aplicada II, Universidad de Sevilla, E-41012 Sevilla, Spain*

[3] *Vice Chancellor, Punjabi University Patiala, 147002, Punjab, India*

We develop a theoretical framework based on a graph theoretic approach to analyze monogamous relationships of entropic non-contextuality (ENC) inequalities. While ENC inequalities are important in quantum information theory and are well studied, theoretical as well as experimental demonstration of their monogamous nature is still elusive. We provide conditions for ENC inequalities to exhibit a monogamous relationship and derive the same for general scenarios. We show that two entropic versions of the Bell-CHSH inequality acting on a tripartite scenario exhibit a monogamous relationship, for which we provide a theoretical proof as well as an experimental validation on an NMR quantum information processor. Our experimental technique to evaluate entropies has been designed to obtain information about entropies via measurement of only the expectation values of observables.

arXiv:2201.02330v2 [quant-ph] 6 Jun 2022

I. INTRODUCTION

It is well known that measurements on quantum states exhibit correlations which defy understanding based on classical theories. The outcomes of measurements performed on spatially separated or even on single indivisible systems may exhibit correlations greater than their apparent classical values. These correlations are termed as Bell non-local [1–4] or contextual [5–9] for bipartite space-like separated and for single indivisible systems respectively, and are studied by means of inequalities, a violation of which implies non-classical behavior [10–14]. The most widely studied of these inequalities include the Bell-CHSH [2] and the KCBS inequality [15], quantifying Bell non-local and contextual correlations, respectively.

Quantum correlations that go beyond the classical allowed values have found immense application in quantum information processing tasks, including self-testing [16, 17], quantum key distribution [18, 19], device independent quantum key distribution [20, 21] and randomness certification [22], to name a few. A common ground of most of these applications is that they utilize the property of monogamy of correlations [23–26]. Such monogamy relations dictate that when two parties are violating a particular inequality (contextual or Bell type), then it is not possible for one of the parties to violate a second similar inequality with a third party on a tripartite state shared amongst all three of them. These monogamy relations have been well studied in the case of Bell inequalities and contextuality [27, 28] Interestingly, monogamous relations also exist between Bell nonlocality and contextuality and these have been verified experimentally [25, 29, 30].

Offering a different perspective on quantum correlations, Braunstein and Caves introduced an information theoretic approach to understand non-local correlations [31, 32] studied in the form of inequalities. These inequalities are eponymously termed as entropic inequalities. In this formalism, the joint Shannon entropies carried by observables must satisfy an inequality in order to have a local description of correlations. This makes the inequalities non-linear functions of probabilities, unlike standard Bell inequalities which are linear. These inequalities are one-way statements; only when an inequality is violated, can it be implied that a joint probability distribution over the observables under consideration cannot exist. However, if the inequality is satisfied, no definite conclusion can be drawn. Subsequently, the work was extended to include non-contextual scenarios [33, 34] as well, and the inequalities are generally termed as entropic non-contextuality (ENC) inequalities. Since their inception, these inequalities have been studied extensively and have also been realized experimentally [35–39]. Experimental implementations of state dependent [38] as well as state independent [39] ENC inequalities have been performed on optical systems.

These ENC inequalities offer an added advantage of being independent of the number of outcomes in a measurement, unlike Bell scenarios where the number of outcomes of a measurement play an important rule in determining the local value. This property of ENC inequalities makes them suitable candidates for applications in nonlocality distillation [34] and bilocality scenarios, among many other applications. Due to their non-linear nature, a general description of monogamous relations for all possible ENC scenarios is a nontrivial task. While there exist scenarios where it is possible to derive a monogamous relationship [32], a generalization of this recipe would be too complex and require involved calculations. There have been attempts in this direction [40] but based on a different approach than ours. Furthermore, while there are a few experimental studies verifying monogamy of

* dileepsingh@iisermohali.ac.in
† jsinghiiser@gmail.com
‡ kavita@iisermohali.ac.in
§ arvind@iisermohali.ac.in

ENC inequalities, all of them are based on optical methods, which are capable of directly yielding probabilities of outcomes of a measurement in the form of frequency of photon detections. However, to the best of our knowledge, there is currently no experimental verification of monogamy of ENC inequalities till date.

Providing a fresh perspective in this paper, we describe an elegant theoretical recipe to evaluate monogamous relations of ENC inequalities and verify the results on an NMR quantum information processor. We develop a theoretical framework, based on graph theoretic formalism, to study monogamous relations of ENC inequalities in arbitrary no-signalling scenarios, apply our formalism to the entropic Bell-CHSH scenario, and derive a monogamous relation between three parties: Alice, Bob and Charlie. We show that if Alice and Bob violate the entropic Bell-CHSH inequality, then Alice and Charlie cannot do so (and vice versa). An added advantage is that our technique also holds for arbitrary m ENC distributed over n parties.

Next we turn to the experimental realization of our results by applying the entropic Bell-CHSH inequality to two different cases. In the first case, all the parties share a mixed tripartite state, such that Alice and Bob share a maximally entangled state with probability p, and Alice and Charlie share the same with probability $1-p$. In the second case, all the parties together share an entangled tripartite pure state. In both the cases, we observe that the monogamous relation is satisfied at all times, while only one of the inequalities is capable of exhibiting a violation. It should be noted that experiments on an NMR quantum information processor only yield an expectation value of the observable, while probabilities of various outcomes cannot be addressed directly. This makes the task of evaluating entropic quantities on this system difficult. To circumvent this difficulty, we provide a novel recipe to evaluate the entropy of an observable on an NMR quantum information processor. In the experiment, all the pure and mixed states were prepared with an experimental fidelity greater than 0.92 and 0.96 respectively, and the experimental results match well with the theoretical predictions.

The paper is organized as follows: in Sec. II A we begin by giving a brief description of entropic inequalities. In Sec. II B we describe our main theoretical result concerning monogamy of ENCs. In Sec. III A we provide an experimental demonstration using a mixed state, while in Sec. III B we use a pure tripartite state for the experiment. Sec. IV contains some concluding remarks.

II. ENTROPIC INEQUALITIES AND THEIR MONOGAMY

In this section we describe our theoretical results, which will be used later in the paper. We begin by providing a brief review of ENC inequalities and focus particularly on the entropic version of the Bell-CHSH inequality.

A. The entropic inequalities

An experiment corresponding to a contextuality inequality can be represented by a graph [41]. Mathematically, a graph G is defined by a set of vertices V and and a set of edges E, such that $G = (V, E)$. In relation to the contextuality inequality, the set V can represent either events, projectors or observables depending upon the scenario, while the set E represents a relationship between different elements of V, such as orthogonality, exclusivity or commutativity [41]. In this paper we use commutativity graphs to study ENC inequalities, in which the set of vertices corresponds to observables and two vertices are connected by an edge if they commute with each other [42].

Consider an n-cycle commutation graph in which the n vertices represent observables X_i and the existence of an edge indicates that the corresponding observables commute. An example of one such graph for $n = 4$ is given in Fig. 2 (top panel).

We assume that a non-contextual joint probability distribution exists over the entire set of observables considered, even though most of them do not commute. It is our aim to construct a condition based on the preceding assumption, for which a violation would indicate that such a non-contextual joint probability distribution does not exist.

The existence of a non-contextual joint probability distribution over the observables X_i implies that it is possible to define a joint Shannon entropy $H(X_0, ..., X_{n-1})$ of them. We can then write

$$H(X_0, X_{n-1}) \leq H(X_0, ..., X_{n-1}), \tag{1}$$

where the relationship $H(X) \leq H(X, Y)$ is physically motivated by the fact that two random variables cannot contain less information than a single one of them. Furthermore, with repeated application of the chain rule $H(X, Y) = H(X|Y) + H(Y)$, where $H(X|Y)$ denotes the conditional entropy of observable X given information about observable Y, the right hand side of the inequality can be re-written as,

$$\begin{aligned} H(X_0,...,X_{n-1}) &\leq H(X_0|X_1,...,X_{n-1}) + H(X_1|X_2,...X_{n-1}) + ... + H(X_{n-2}|X_{n-1}) + H(X_{n-1}) \\ &\leq H(X_0|X_1) + H(X_1|X_2) + ... + H(X_{n-2}|X_{n-1}) + H(X_{n-1}). \end{aligned} \tag{2}$$

The latter inequality in Eq. (2) is a consequence of the relationship $H(X|Y) \leq H(X)$, which implies that conditioning cannot increase the information content of a random variable. Plugging Eq. (2) in Eq. (1) and using $H(X_0|X_{n-1}) = H(X_0, X_{n-1}) - H(X_{n-1})$, we finally get the required entropic non-contextuality inequality,

$$H_{K_1} : H(X_0|X_{n-1}) \leq H(X_0|X_1) + ...H(X_{n-2}|X_{n-1}). \tag{3}$$

A violation of Eq. (3) would then indicate that a non-contextual joint probability distribution over the corresponding set of observables does not exist.

It should be noted that no assumptions have been made regarding the nature of the observables X_i. For all intents and purposes they can correspond to projective measurements or POVMs with any number of outcomes. Furthermore, the observables could correspond to local scenarios or non-local, in which case the entropic inequality would be termed as non-contextual or Bell non-local. Since we consider generalized scenarios, we term all entropic inequalities as non-contextual as it subsumes the non-local scenarios as well.

One of the many interesting cases arises for $n = 4$ observables, which corresponds to the well known Bell-CHSH scenario. Consider two parties, Alice and Bob, each having two observables labelled $\{A_0, A_1\}$ and $\{B_0, B_1\}$ respectively, such that observables of any one party do not commute, while observables of different parties commute. Differing from the traditional Bell-CHSH scenario, it is also assumed that a measurement of the observables can have an arbitrary number of outcomes. The corresponding entropic inequality is written as,

$$H_{K_1} : H(A_1|B_1) - H(A_1|B_0) - H(B_0|A_0) - H(A_0|B_1) \leq 0. \tag{4}$$

A violation of the above inequality implies a non-existence of a joint probability distribution over all the observables A_x and B_y $\forall x, y \in \{0, 1\}$. In the next section, we show that ENC inequalities admit a monogamous relationship which can be derived using a graph theoretic formalism. We particularly focus on the entropic Bell-CHSH scenario described above and show that it admits a monogamous relationship.

B. Monogamy of entropic inequalities

We now elucidate the formalism to check and derive a monogamous relationship for any arbitrary scenario using the graph theoretic formalism. It should be remembered that a violation of the inequality (4) implies that a joint probability distribution cannot exist over the given observables.

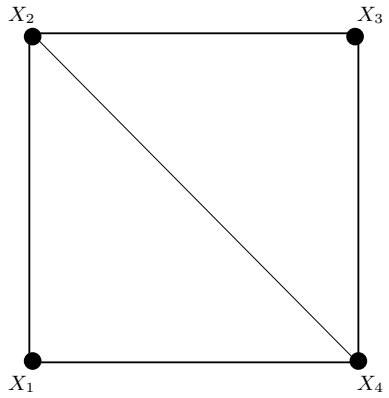


FIG. 1. The chordal subgraph where the vertices represents observables X_i with $i = 1, 2, 3, 4$ and the edge indicate commutativity relationship between the observables.

Proposition 1. *A monogamous relationship for a set of n observables X_i, corresponding to m non-contextuality scenarios exists if their joint commutation graph can be vertex decomposed into m chordal subgraphs such that all edges appearing in the original m non-contextuality graphs must appear just once in the decomposition. The monogamous relationship then reads as,*

$$H_{K_1} + H_{K_2} + H_{K_3} + ... + H_{K_m} \leq 0, \tag{5}$$

where H_{K_i} denotes the ith ENC inequality.

Proof. A chordal graph is a graph in which all cycles of four or more vertices have a chord. A chord is an edge that is not part of the cycle but which connects two of the vertices. It should be noted that the definition of chordal subgraphs implies that these subgraphs must have an edge connecting two vertices, such that any induced cycles in the subgraph have a length equal to three. Any induced cycles of length greater than 3 should then have an edge such that the resultant induced cycle satisfies the definition.

For these 3-cycle induced subgraphs, it is possible to write down the corresponding entropic inequality. Since it is a 3-cycle graph, a joint probability distribution over the observables always exists [28] and the entropic inequality is never violated. Therefore, we can add all the entropic inequalities obtained in this fashion to obtain

$$\sum_l \sum_{i,j=1}^{n} g_l(H'(X_i|X_j)), \tag{6}$$

where $H'(X_i|X_j) = H(X_i|X_j)$ only if the vertices i and j belong to an edge and zero otherwise, $g(X) = \pm X$ depending on the 3 cycle chosen and l is the number of edges

appearing in the m chordal graphs. It should be noted that Eq. (6) is a linear combination of $H(X_i|X_j)$ and since we require that all the terms appearing in the individual m ENC inequalities appear in the decomposition, it is possible to obtain the form in Eq. (5) via linear manipulation of the ENC inequalities of the 3-cycle induced graphs. It should be noted that each term appearing in Eq. (3) corresponds to an edge in the commutativity graph and missing even a single edge in the chordal decomposition, would make one of the non-contextuality inequalities incomplete and Eq. (5) unachievable. Furthermore, the linear manipulations required correspond to choosing a suitable form of $g(X)$ such that the m ENC inequalities can be obtained by grouping certain terms together. This manipulation depends on the commutation graph of the interested scenario.

As an example of our technique consider the chordal graph given in Fig. 1 which is formed by two 3-cycle graphs. We assume that this is one of the subgraphs obtained via vertex decomposition of a joint commutativity graph such that the term $H(X_2|X_4)$ corresponding to the edge (X_2, X_4) does not appear in Eq. (5), while the terms corresponding to the other edges do appear. In order to eliminate this term, we consider the ENC inequality for the 3-cycle graph with vertices (X_1, X_2, X_4), written in a cyclic form as,

$$H(X_1|X_4) - H(X_1|X_2) - H(X_2|X_4) \leq 0, \tag{7}$$

while for the other 3-cycle graph formed by the vertices (X_2, X_3, X_4) we use an anti-cyclic form of the ENC inequality as,

$$H(X_2|X_4) - H(X_2|X_3) - H(X_3|X_4) \leq 0. \tag{8}$$

Since all 3-cycle graphs admit a joint probability distribution, the aforementioned inequalities are always satisfied and can therefore be added to give,

$$H(X_1|X_4) - H(X_1|X_2) - H(X_2|X_3) - H(X_3|X_4) \leq 0, \tag{9}$$

which is the ENC inequality over the graph in Fig 1 without the edge (X_2, X_4). We use this technique to derive our monogamous relationships. In the case when such a vertex decomposition cannot be found, we cannot guarantee that a monogamous relation will exist.

We now apply this technique to derive a monogamous relationship of two entropic CHSH inequalities. Consider a standard monogamous relationship between two entropic non-contextuality scenarios, K_1 and K_2 which should dictate,

$$H_{K_1} + H_{K_2} \leq 0, \tag{10}$$

where $H_{K_{1(2)}} \leq 0$ denotes the existence of a joint probability distribution over the n observables. Since the monogamy relationship must be obeyed at all times, Eq. (10) then physically implies that a joint probability distribution over all the observables appearing in the new entropic inequality, $H = H_{K_1} + H_{K_2}$ exists.

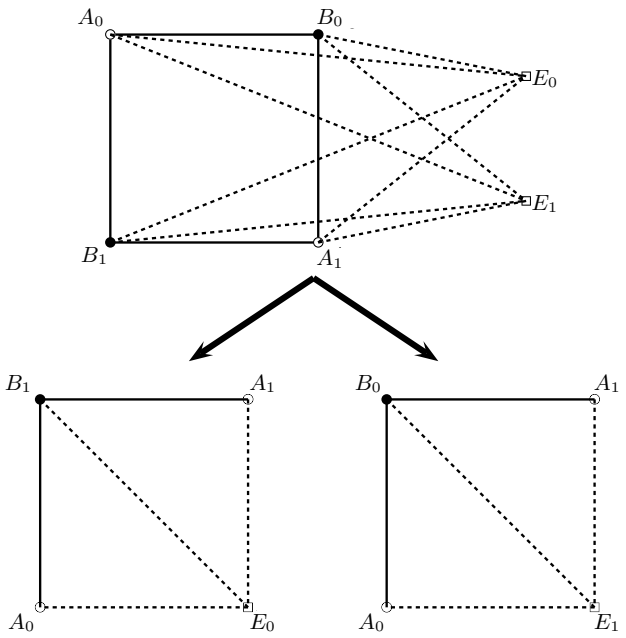


FIG. 2. The joint commutation graph of Alice-Bob-Eve (top) and its chordal decomposition (below) according to Proposition 1, where solid lines indicate commutativity between observables of Alice and Bob, while dashed lines indicate commutativity between Alice (Bob) and Charlie.

As explained, in order to achieve a form of Eq. (10), the joint graph of the non-contextuality scenarios must be decomposable into chordal subgraphs, which admit a joint probability distribution. However, we also require an additional feature that all edges of the individual non-contextuality graphs must appear at least once in any of the chordal subgraphs.

Consider the CHSH scenario in which two parties Alice and Bob can perform a measurement of the observables A_0, A_1 and B_0, B_1 respectively. We assume a third party Charlie with observables E_0 and E_1, which commute with the observables of Alice and Bob. The scenario is illustrated by a joint graph as shown in Fig. 2, where vertices represent observables and edges indicate the commutation relationship. Without loss of generality we assume that Charlie would like to violate the entropic CHSH inequality with Alice. The two corresponding Alice-Bob and Alice-Charlie entropic CHSH inequalities are,

$$\begin{aligned} H_{K_1} :& H(A_0|B_0) - H(A_0|B_1) \\ & - H(B_1|A_1) - H(A_1|B_0) \leq 0, \end{aligned} \tag{11}$$

$$\begin{aligned} H_{K_2} :& H(A_0|E_0) - H(A_0|E_1) \\ & - H(E_1|A_1) - H(A_1|E_0) \leq 0. \end{aligned} \tag{12}$$

The joint commutation graph is decomposed into two chordal graphs while keeping the edges appearing in the individual Alice-Bob and Alice-Charlie CHSH scenarios

intact in the decomposition, as shown in Fig. (2). The corresponding ENC inequalities for each 3-cycle graph in every chordal subgraph are given as,

$$H(A_0|E_0) - H(A_0|B_1) - H(B_1|E_0) \leq 0, \quad (13)$$
$$H(B_1|E_0) - H(B_1|A_1) - H(A_1|E_0) \leq 0, \quad (14)$$
$$H(A_0|B_0) - H(A_0|E_1) - H(E_1|B_0) \leq 0, \quad (15)$$
$$H(E_1|B_0) - H(E_1|A_1) - H(A_1|B_0) \leq 0, \quad (16)$$

Being cyclic and chordal, all the above inequalities are a necessary and sufficient condition for a joint probability distribution to exist. Furthermore, we have carefully chosen the terms with positive and negative coefficients so as to achieve a final form according to Eq. (10). Adding the above inequalities and grouping the terms according to H_{K_1} and H_{K_2}, we obtain

$$H_{K_1} + H_{K_2} \leq 0, \quad (17)$$

which is the required monogamy relationship. We note that this monogamy relationship was also derived in [32], albeit in a different manner and specifically for the entropic CHSH inequality. However, our formalism can be readily generalized to n observables distributed among m parties. □

The derived monogamy relationship (17) imposes severe restrictions on the violation of Alice-Charlie entropic CHSH inequality.

III. EXPERIMENTAL DEMONSTRATION

In this section, we experimentally demonstrate the monogamy relationship derived for the entropic Bell-CHSH scenario (17) on an NMR quantum information processor, using two different set of states. We show that for both the sets of states, the entropic Bell-CHSH obeys the monogamy relationship we derived above.

A. Implementation using a mixed tripartite state

We experimentally implement the monogamy inequality (17) using a mixed tripartite state which is a classical mixture of two pure maximally entangled states given as:

$$\rho = p(|\psi_1\rangle\langle\psi_1|) + (1-p)(|\psi_2\rangle\langle\psi_2|), \quad (18)$$

where

$$|\psi_1\rangle = \frac{1}{\sqrt{2}}(|001\rangle + |111\rangle),$$
$$|\psi_2\rangle = \frac{1}{\sqrt{2}}(|010\rangle + |111\rangle), \quad (19)$$

and $p \in [0,1]$. As can be seen, the state ρ physically implies that Alice and Bob share a maximally entangled state with probability p while Charlie is separable, and with probability $1-p$, Alice and Charlie share a maximally entangled state while Bob is separable.

The observables of Alice, Bob and Charlie are assumed to lie in the $X-Z$ plane and correspond to Pauli spin measurements along the unit vectors $\boldsymbol{a}, \boldsymbol{a'}, \boldsymbol{b}, \boldsymbol{b'}$ and $\boldsymbol{e}, \boldsymbol{e'}$ respectively. The vectors $\boldsymbol{a}, \boldsymbol{b'}, \boldsymbol{a'}$ and $\boldsymbol{b}$ are successively separated by an angle $\frac{\theta}{3}$, while the vectors $\boldsymbol{e}$ and $\boldsymbol{e'}$ are taken to be the same as Bob's. The corresponding Pauli observables are then given as:

$$A_0 = \begin{bmatrix} 1 & 0 \\ 0 & -1 \end{bmatrix}, \quad A_1 = \begin{bmatrix} \cos\frac{2\theta}{3} & -\sin\frac{2\theta}{3} \\ \sin\frac{2\theta}{3} & \cos\frac{2\theta}{3} \end{bmatrix}$$
$$B_0 = \begin{bmatrix} \cos\theta & -\sin\theta \\ \sin\theta & \cos\theta \end{bmatrix}, \quad B_1 = \begin{bmatrix} \cos\frac{\theta}{3} & -\sin\frac{\theta}{3} \\ \sin\frac{\theta}{3} & \cos\frac{\theta}{3} \end{bmatrix}, \quad (20)$$

while the observables of Charlie (E_0, E_1) are the same as Bob's but acting in a different Hilbert space. All of the aforementioned observables have eigenvalues $a_i, b_i, e_i \in \{-1, +1\}$ and follow the commutativity conditions as shown in Fig. 2.

For the set of observables given in Eq. (20), the maximum violation of the Alice-Bob entropic CHSH inequality $H_{K1} = 0.237$ bits is found to be at $\theta = 0.457$ radians when the parties share the state $|\psi_1\rangle$. The same also holds for Alice-Charlie entropic CHSH inequality when the parties share the state $|\psi_2\rangle$.

We experimentally implemented the monogamy relation given in Eq. (17) on an eight-dimensional quantum system. We used a molecule of ^{13}C -labeled diethyl fluoromalonate dissolved in acetone-D6, with the ^{1}H, ^{19}F and ^{13}C spin-1/2 nuclei being encoded as 'qubit one', 'qubit two' and 'qubit three', respectively (see Fig. 3(a)). The system was initialized in the pseudopure state (PPS) $|000\rangle$ using the spatial averaging technique [43] and the corresponding NMR spectra and experimental tomographs are given in Fig. 3(a),(b).

Experiments were performed on a Bruker Avance III 600-MHz FT-NMR spectrometer equipped with a QXI probe. Local unitary operations were achieved by RF pulses of suitable amplitude, phase, and duration and nonlocal unitary operations were achieved by free evolution under the system Hamiltonian. The T_1 and T_2 relaxation times of ^{1}H, ^{19}F, ^{13}C spin-1/2 nuclei range from 4.16 sec to 7.16 sec and 0.99 sec to 3.56 sec, respectively. The duration of the $\frac{\pi}{2}$ pulses for ^{1}H, ^{19}F, and ^{13}C nuclei are 9.5 μs at 18.14 W power level, 22.2 μs at a power level of 42.27 W, and 15.2 μs at a power level of 179.47 W, respectively. At room temperature, NMR experiments are only sensitive to the deviation density matrix and the initial state is prepared from the thermal equilibrium into a PPS:

$$\rho_{000} = \frac{1-\epsilon}{2^3} I_8 + \epsilon|000\rangle\langle 000| \quad (21)$$

where $\epsilon \approx 10^{-6}$ and I_8 is 8×8 identity operator. The system is initialized in the PPS state *i.e.*$|000\rangle$ using the

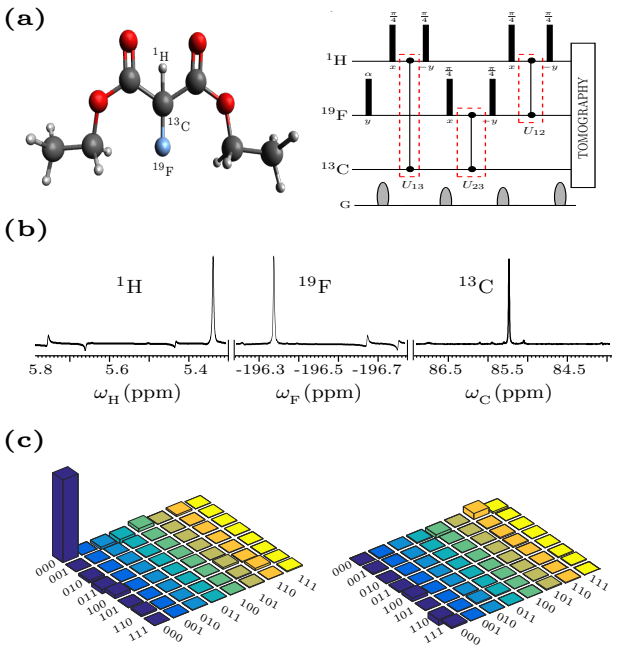


FIG. 3. (a) Molecular structure of ^{13}C - labeled diethyl fluoromalonate. ^{1}H, ^{19}F, ^{13}C are used as three qubits in the experiment. NMR pulse sequence for the initialization of the state into the PPS $|000\rangle$ state. The value of the flip angle α is kept at 57.87°. The phases and the flip angles are written with each pulse. The U_{12}, U_{23}, U_{13} are evolution operators with time intervals τ_{12}, τ_{23}, τ_{13} equal to $\frac{1}{2J_{HF}}$, $\frac{1}{2J_{HC}}$, and $\frac{1}{2J_{FC}}$ respectively, shown by red dotted lines. (b) The NMR spectra corresponding to the PPS $|000\rangle$. The horizontal scale represents the chemical shifts in ppm. (c) Real (left) and imaginary (right) parts of the experimentally reconstructed tomographs of the state $|000\rangle$ with an experimental state fidelity of 0.98.

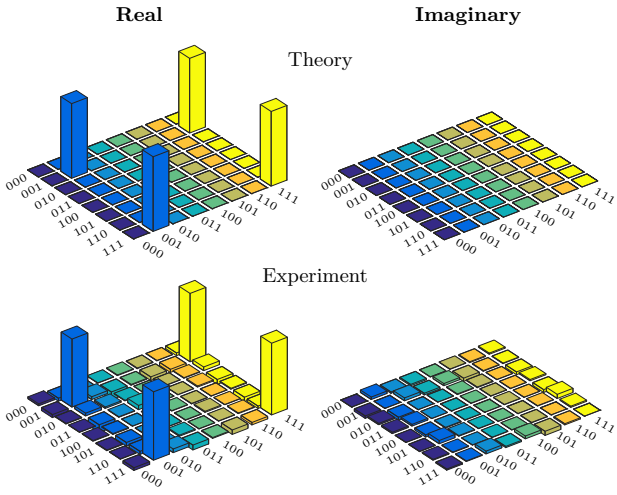


FIG. 4. Real and imaginary parts of the tomographs of the theoretically and experimentally reconstructed density operator for the tripartite state ρ with $p = 1$ and an experimental state fidelity of 0.97.

spatial averaging technique [43], which is based on dividing the system in sub-ensembles which can be accessed independently in NMR by using a combination of RF pulses and pulsed magnetic gradients. The state tomography was performed using the least square optimization technique[44] with an experimental state fidelity of 0.98.

We began by preparing the mixed tripartite state given in Eq. (18) for different values of p. In order to achieve this, we utilized the temporal averaging technique [45, 46]. Using this technique, it is possible to prepare arbitrary mixed states on an NMR quantum information processor, by applying suitable unitary transformations on some common initial PPS. The different experiments are performed on common initial states, the results of which are independently stored. Finally, these results are combined to produce an average state which simulates the behavior of a mixed state.

In our case, we prepared the mixed state given in Eq. (18), which is a mixture of two pure states $|\psi_1\rangle$, $|\psi_2\rangle$. We first prepared these two states by applying suitable unitaries on the initial state $|000\rangle\langle 000|$ in two different and independent experiments [47]. The states of these two experiments are then added with appropriate probabilities to achieve the desired mixed state given in Eq. (18). To demonstrate the monogamy relation, we chose different values of p to experimentally prepare the desired mixed state with experimental state fidelities ≥ 0.956. The tomograph of one such experimentally prepared state with $p = 1$ is shown in Fig. 4.

After experimentally preparing the states, we measured the desired probabilities in order to calculate the entropies involved in the inequality given in Eq. (17). In order to calculate the probabilities, we transformed the required probabilities in terms of expectation values. This is necessary because experiments on an NMR quantum information processor yield only expectation values of the observables. These expectation values are evaluated by decomposing the observables in terms of linear combinations of Pauli operators which can be mapped to the single-qubit Pauli Z operator. This mapping is particularly useful in the context of an NMR experimental setup where the expectation value of the Z operator is easily accessible and corresponds to the observed z magnetization of a nuclear spin in a particular quantum state. The normalized experimental intensities of the NMR signal then provide an estimate of the expectation value of the Pauli Z operator in that quantum state [48].

The probabilities can be written as $P(A_i = a_i, B_j = b_j) = \mathrm{tr}(\rho|a_i\rangle\langle a_i| \otimes |b_j\rangle\langle b_j| \otimes I)$ and $P(A_i = a_i, E_j = e_j) = \mathrm{tr}(\rho|a_i\rangle\langle a_i| \otimes I \otimes |e_j\rangle\langle e_j|)$ where $|a_i\rangle$, $|b_j\rangle$, $|e_j\rangle$ are the eigenvector of the observables corresponding to Alice, Bob and Charlie, respectively. The observables $(|a_i\rangle\langle a_i| \otimes |b_j\rangle\langle b_j| \otimes I)$, $(|a_i\rangle\langle a_i| \otimes I \otimes |e_i\rangle\langle e_i|)$ are decomposed in terms of linear combinations of Pauli operators and details are given in Appendix-A. The idea is to unitarily map the state ρ to another state ρ', such that

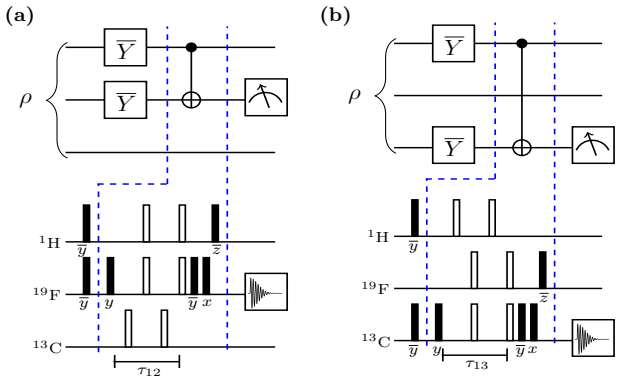


FIG. 5. Quantum circuit and corresponding NMR pulse sequence to map the state ρ to the state ρ' such that (a) $\langle \sigma_x \otimes \sigma_x \otimes I \rangle_\rho = \langle I_{2z} \rangle_{\rho'}$, (b) $\langle \sigma_x \otimes I \otimes \sigma_x \rangle_\rho = \langle I_{3z} \rangle_{\rho'}$. In the NMR pulse sequences, the filled rectangles are $\frac{\pi}{2}$ RF pulses while unfilled rectangles denotes the π RF pulses. The phase of each pulse is written over the respective pulse and bar over the phase denotes the negative phase. The free evolution of time is denoted by τ_{12}, τ_{13}.

$\langle X \rangle_\rho = \langle I_{iz} \rangle_{\rho'}$ where X is the observable to be measured in the state ρ and I_{iz} is the z-spin angular momentum of the qubit. This can be achieved by measuring the I_{iz} on the state ρ'. For example, one can find the expectation values of $\langle \sigma_x \otimes \sigma_x \otimes I \rangle_\rho$ and $\langle \sigma_x \otimes I \otimes \sigma_x \rangle_\rho$ which are involved in the evaluation of probabilities (see Appendix-A), by using the quantum circuit and corresponding NMR pulse sequence given in Fig.5(a) and Fig.5(b) respectively, where the implementation is followed by a measurement of the spin magnetization of the second and third qubits, respectively.

We experimentally calculated the ENC inequalities H_{K1}, H_{K2} and the ENC monogamy relation $H_{K1} + H_{K2}$ for the tripartite mixed state given in Eq. (18) for different values of p. Experimental values of H_{K1}, H_{K2}, $H_{K1} + H_{K2}$ with respect to various values of p are plotted in Fig. 6. It can be seen that H_{K1} is violated for the tripartite state with $p = 1$, while H_{K2} is violated for the state with $p = 0$. The monogamy relation $H_{K1} + H_{K2}$ is never violated for any value of p and the results are in good agreement with the theoretical predictions.

It is seen that the experimental values are always lower than the corresponding theoretical values. This is due to the fact that the maximum value of the inequality is always achieved for a pure state and any addition of noise makes it a mixed state. Therefore, the value is always observed to be lower than the theoretical one. The difference between them also increases with increasing values of p upto $p = 0.5$. For this region, the state prepared for $p = 0.0$ is the dominant one which is shown to violate H_{K_1}. Furthermore, the corresponding inequalities are logarithmic in nature, which also compounds the errors for states till $p = 0.5$. However, after this value the state prepared for $p = 1.0$ dominates and the errors again follow a similar trend. It should be noted that the experimental curve follows the same trend as the theoretical curve.

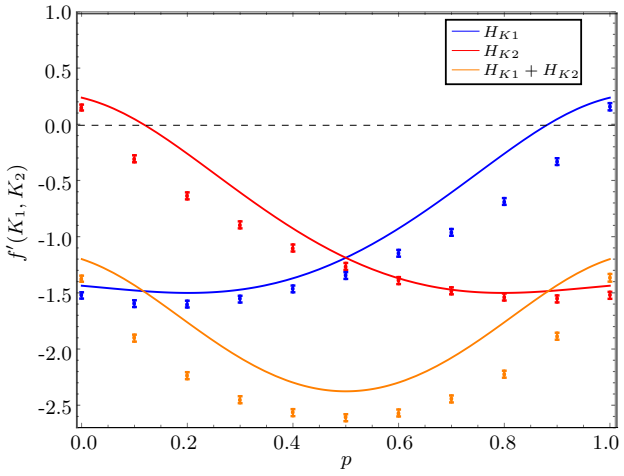


FIG. 6. The experimentally calculated values for the monogamy inequality Eq. (17) denoted by $f'(K_1, K_2)$ for the tripartite mixed states given in Eq. (18) for different values of p. The black dotted line is the maximum non-contextual value that can be achieved by inequalities H_{K1}, H_{K2} and $H_{K1} + H_{K2}$ to follow the ENC theories and monogamy relationship, respectively. The red color line and the red points with error bars represent the theoretical and experimental calculated values for the inequality H_{K1}, respectively. Similar representations for the inequalities H_{K2} and $H_{K1} + H_{K2}$ are used.

B. Implementation using a pure tripartite state

In this subsection, we experimentally test the monogamy relation Eq. (17) for a pure tripartite state, having two parameters which we can vary. We show that the monogamy relation holds and is in good agreement with theoretical predictions.

We take a pure tripartite state of the form,

$$|\phi\rangle = N(p_1|001\rangle + p_2|010\rangle + (p_1 + p_2)|111\rangle), \qquad (22)$$

where $N = \frac{1}{\sqrt{p_1^2 + p_2^2 + (p_1+p_2)^2}}$ is the normalization factor. We experimentally prepared five different states corresponding to various values of p_1 and p_2. The quantum circuit and the corresponding NMR pulse sequence is given in Fig. 7(a), (b). Different pure states corresponding to various values of p_1 and p_2 were generated by suitably choosing the values of θ_1, θ_2 and θ_3. Tomograph of one such experimentally prepared state with $p_1 = 0.25$ and $p_2 = 0.50$ is depicted in Fig. 8, with an experimental state fidelity of 0.93. After preparing the states, we measured the desired probabilities by mapping the state onto the Pauli basis operators in order to calculate the entropies involved in the inequality Eq. (17) as discussed earlier in Sec. III A.

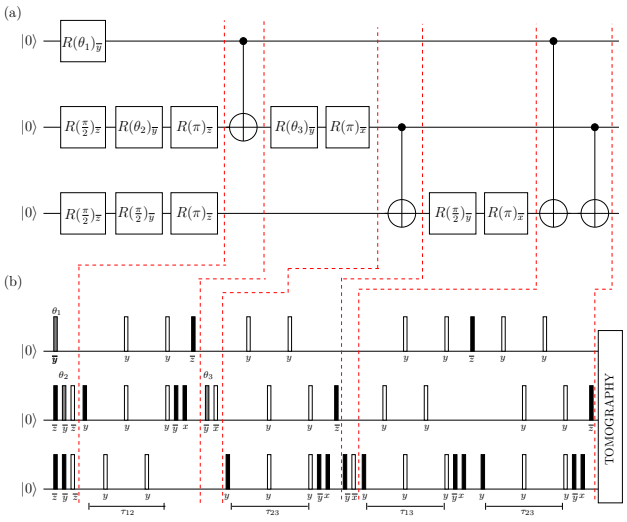


FIG. 7. (a) Quantum circuit for state preparation for the tripartite pure state $|\phi\rangle$ and (b) corresponding NMR pulse sequence. The filled rectangles denote $\frac{\pi}{2}$ RF pulses while the unfilled rectangles denote π RF pulses. The phase of each pulse is written over the respective pulse, and bar over the phase denotes a negative phase. $\tau_{12}, \tau_{23}, \tau_{13}$ are the free time evolutions. All the CNOTS are separated by red dotted lines.

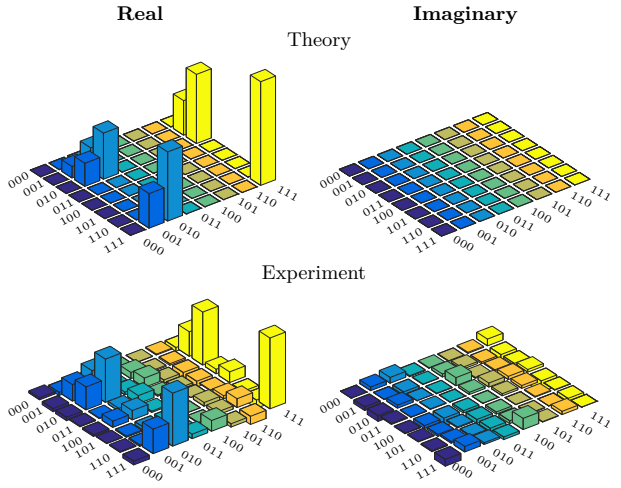


FIG. 8. Real and imaginary part of tomograph of the theoretically and experimentally reconstructed density operator for the tripartite pure state $\rho' = |\phi\rangle\langle\phi|$ with $p_1 = 0.25, p_2 = 0.50$ with an experimental state fidelity of 0.93.

We experimentally evaluate H_{K_1}, H_{K_2} and $H_{K_1} + H_{K_2}$ with respect to the different values of p_1 and p_2 and the results are given in Table-I. We see that the inequality H_{K_1} is violated for $p_1 = 1$ and $p_2 = 0$ and H_{K_2} is violated for $p_1 = 0$ and $p_2 = 1$, while the monogamy relationship $H_{K_1} + H_{K_2}$ is never violated for any value of p_1 and p_2. This shows that the monogamy relation between the ENC inequalities is obeyed for all such possible states.

IV. CONCLUDING REMARKS

In this paper we develop a theoretical framework to analyze when a scenario will exhibit a monogamous relationship. We perform our analysis of the monogamy relations expected in a general tripartite scenario for the entropic Bell-CHSH inequality and give the first theoretical study of the monogamy of entropic inequalities based on the graph theoretic formalism. We also give the first experimental demonstration of monogamy of entropic correlations using three NMR qubits. Evaluating entropy on an NMR quantum processor is quite hard and has not been performed earlier. We are able to obtain information about entropies using measurements of only the expectation values of observables. We experimentally show the monogamy of entropic inequality for a pure tripartite state as well as for the mixed state. This indicates with certainty that our formalism holds in general.

It should be noted that due to limitations of access to individual events, the NMR implementation of such scenarios involves use of Born rule to interpret the results of measurements. This is not the ideal way of carrying out such experiments and a more refined test would evaluate the requisite probabilities without assuming the Born rule. This is possible on optical systems [38, 39], where the probabilities are calculated by estimating the frequency clicks of the photodetectors rather than the Born rule.

The experimental implementation of monogamy inequalities is important for quantum information processing tasks and our results are a step forward in this direction.

ACKNOWLEDGMENTS

All the experiments were performed on a Bruker Avance-III 600 MHz FT-NMR spectrometer at the NMR Research Facility of IISER Mohali. A. acknowledges financial support from DST/ICPS/QuST/Theme-1/2019/Q-68. K .D. acknowledges financial support from DST/ICPS/QuST/Theme-2/2019/Q-74. JS acknowledges support by Universidad de Sevilla Project Qdisc (Project No. US-15097), with FEDER funds, MCINN/AEI Projet No. PID2020-113738GB-I00, and QuantERA grant SECRET, by MCINN/AEI (Project No. PCI2019-111885-2).

Appendix A: Observable decomposition in terms of Pauli operators

To experimentally test the inequality on an NMR quantum processor, we have calculated the entropies involved in the inequality by measuring the probabilities for an experimentally prepared state. This can be achieved by decomposing the projectors $|a_{\pm 1}\rangle\langle a_{\pm 1}| \otimes |b_{\pm 1}\rangle\langle b_{\pm 1}|$ as linear combinations of Pauli operators, which can then be

TABLE I. Theoretically computed and experimentally measured values of the monogamy inequalities for a pure state.

		H_{K_1}		H_{K_2}		$H_{K_1}+H_{K_2}$	
p_1	p_2	Theory	Experiment	Theory	Experiment	Theory	Experiment
1.00	0.00	0.236	0.156±0.032	-1.436	-1.522±0.035	-1.200	-1.366±0.034
0.50	0.25	-0.492	-0.606±0.021	-1.338	-1.413±0.027	-1.830	-2.019±0.024
0.50	0.50	-1.017	-1.103±0.022	-1.017	-1.082±0.030	-2.034	-2.185±0.026
0.25	0.50	-1.338	-1.397±0.021	-0.492	-0.598±0.024	-1.830	-1.995±0.023
0.00	1.00	-1.436	-1.523±0.028	0.236	0.149±0.025	-1.200	-1.374±0.027

mapped to a single-qubit Pauli Z operator. In the tripartite scenario, the probabilities can be written as $P(A_i = \pm1, B_j = \pm1) = \mathrm{tr}(\rho|a_{\pm1}\rangle\langle a_{\pm1}| \otimes |b_{\pm1}\rangle\langle b_{\pm1}| \otimes I)$ and $P(A_i = \pm1, E_j = \pm1) = \mathrm{tr}(\rho|a_{\pm1}\rangle\langle a_{\pm1}| \otimes I \otimes |e_{\pm1}\rangle\langle e_{\pm1}|)$ for the Alice-Bob and Alice-Charlie entropic CHSH inequalities. To test the monogamy inequality Eq.(17), we measure the probabilities to calculate the entropies $H(A_i|B_j)$ $H(A_i|E_j)$ involved in the inequalities H_{K1} and H_{K2}.

Probabilities are calculated by decomposing the observables in terms of linear combination of Pauli operators as:

$$
\begin{aligned}
\mathrm{P(A_1 = +1)} &= 0.286\mathrm{b_{16}} + 0.410\mathrm{b_{48}} + 0.500I,\\
\mathrm{P(B_1 = +1)} &= 0.476\mathrm{b_{12}} + 0.149\mathrm{b_4} + 0.500I,\\
\mathrm{P(A_0 = +1,\, B_0 = +1)} &= 0.152b_{12} + 0.197\mathrm{b_4} + 0.250\mathrm{b_{48}}\\
&\quad + 0.197\mathrm{b_{52}} + 0.152\mathrm{b_{60}} + 0.250I,\\
\mathrm{P(A_0 = +1,\, B_0 = -1)} &= -0.152\mathrm{b_{12}} - 0.197\mathrm{b_4} + 0.250\mathrm{b_{48}}\\
&\quad - 0.197\mathrm{b_{52}} - 0.152\mathrm{b_{60}} + 0.250I,\\
\mathrm{P(A_0 = -1,\, B_0 = +1)} &= 0.152\mathrm{b_{12}} + 0.197\mathrm{b_4} - 0.250\mathrm{b_{48}}\\
&\quad - 0.197\mathrm{b_{52}} - 0.152\mathrm{b_{60}} + 0.250I,\\
\mathrm{P(A_0 = -1,\, B_0 = -1)} &= -0.152\mathrm{b_{12}} - 0.197\mathrm{b_4} - 0.250\mathrm{b_{48}}\\
&\quad + 0.197\mathrm{b_{52}} + 0.152\mathrm{b_{60}} + 0.250\mathrm{I},\\
\mathrm{P(A_0 = +1,\, B_1 = +1)} &= 0.238\mathrm{b_{12}} + 0.074\mathrm{b_4} + 0.250\mathrm{b_{48}}\\
&\quad + 0.074\mathrm{b_{52}} + 0.238\mathrm{b_{60}} + 0.250I,\\
\mathrm{P(A_0 = +1,\, B_1 = -1)} &= -0.238\mathrm{b_{12}} - 0.074\mathrm{b_4} + 0.250\mathrm{b_{48}}\\
&\quad - 0.074\mathrm{b_{52}} - 0.238\mathrm{b_{60}} + 0.250I,\\
\mathrm{P(A_0 = -1,\, B_1 = +1)} &= 0.238\mathrm{b_{12}} + 0.074\mathrm{b_4} - 0.250\mathrm{b_{48}}\\
&\quad - 0.074\mathrm{b_{52}} - 0.238\mathrm{b_{60}} + 0.250I,\\
\mathrm{P(A_0 = -1,\, B_1 = -1)} &= -0.238\mathrm{b_{12}} - 0.074\mathrm{b_4} - 0.250\mathrm{b_{48}}\\
&\quad + 0.074\mathrm{b_{52}} + 0.238\mathrm{b_{60}} + 0.250I,
\end{aligned}
\tag{A1}
$$

$$
\begin{aligned}
\mathrm{P(B_1 = +1,\, A_1 = +1)} &= 0.205\mathrm{b_{12}} + 0.074\mathrm{b_{16}} + 0.042\mathrm{b_{20}}\\
&\quad + 0.061\mathrm{b_{28}} + 0.143\mathrm{b_4} + 0.238\mathrm{b_{48}}\\
&\quad + 0.136\mathrm{b_{52}} + 0.195\mathrm{b_{60}} + 0.250I,\\
\mathrm{P(B_1 = +1,\, A_1 = -1)} &= -0.205\mathrm{b_{12}} + 0.074\mathrm{b_{16}} - 0.042\mathrm{b_{20}}\\
&\quad - 0.061\mathrm{b_{28}} - 0.143\mathrm{b_4} + 0.238\mathrm{b_{48}}\\
&\quad - 0.136\mathrm{b_{52}} - 0.195\mathrm{b_{60}} + 0.250I,\\
\mathrm{P(B_1 = -1,\, A_1 = +1)} &= 0.205\mathrm{b_{12}} - 0.074\mathrm{b_{16}} - 0.042\mathrm{b_{20}}\\
&\quad - 0.061\mathrm{b_{28}} + 0.143\mathrm{b_4} - 0.238\mathrm{b_{48}}\\
&\quad - 0.136\mathrm{b_{52}} - 0.195\mathrm{b_{60}} + 0.250I,\\
\mathrm{P(B_1 = -1,\, A_1 = -1)} &= -0.205\mathrm{b_{12}} - 0.074\mathrm{b_{16}} + 0.042\mathrm{b_{20}}\\
&\quad + 0.061\mathrm{b_{28}} - 0.143\mathrm{b_4} - 0.238\mathrm{b_{48}}\\
&\quad + 0.136\mathrm{b_{52}} + 0.195\mathrm{b_{60}} + 0.250I,
\end{aligned}
\tag{A2}
$$

$$
\begin{aligned}
\mathrm{P(A_1 = +1,\, B_0 = +1)} &= 0.152\mathrm{b_{12}} + 0.143\mathrm{b_{16}} + 0.113\mathrm{b_{20}}\\
&\quad + 0.078\mathrm{b_{28}} + 0.197\mathrm{b_4} + 0.205\mathrm{b_{48}}\\
&\quad + 0.162\mathrm{b_{52}} + 0.125\mathrm{b_{60}} + 0.250I,\\
\mathrm{P(A_1 = +1,\, B_0 = -1)} &= -0.152\mathrm{b_{12}} + 0.143\mathrm{b_{16}} - 0.113\mathrm{b_{20}}\\
&\quad - 0.078\mathrm{b_{28}} - 0.197\mathrm{b_4} + 0.205\mathrm{b_{48}}\\
&\quad - 0.162\mathrm{b_{52}} - 0.125\mathrm{b_{60}} + 0.250I,\\
\mathrm{P(A_1 = -1,\, B_0 = +1)} &= 0.152\mathrm{b_{12}} - 0.143\mathrm{b_{16}} - 0.113\mathrm{b_{20}}\\
&\quad - 0.078\mathrm{b_{28}} + 0.197\mathrm{b_4} - 0.205\mathrm{b_{48}}\\
&\quad - 0.162\mathrm{b_{52}} - 0.125\mathrm{b_{60}} + 0.250I,\\
\mathrm{P(A_1 = -1,\, B_0 = -1)} &= -0.152\mathrm{b_{12}} - 0.143\mathrm{b_{16}} + 0.113\mathrm{b_{20}}\\
&\quad + 0.078\mathrm{b_{28}} - 0.197\mathrm{b_4} - 0.205\mathrm{b_{48}}\\
&\quad + 0.162\mathrm{b_{52}} + 0.125\mathrm{b_{60}} + 250I.
\end{aligned}
\tag{A3}
$$

$$
\begin{aligned}
\mathrm{P}(\mathrm{A}_1=+1) &= 0.286\mathrm{b}_{16}+0.410\mathrm{b}_{48}+0.500I,\\
\mathrm{P}(\mathrm{E}_1=+1) &= 0.149\mathrm{b}_{1}+0.476\mathrm{b}_{3}+0.500I,\\
\mathrm{P}(\mathrm{A}_0=+1,\,\mathrm{E}_0=+1) &= 0.197\mathrm{b}_{1}+0.152\mathrm{b}_{3}+0.250\mathrm{b}_{48}\\
&\quad+0.197\mathrm{b}_{49}+0.152\mathrm{b}_{51}+0.250I,\\
\mathrm{P}(\mathrm{A}_0=+1,\,\mathrm{E}_0=-1) &= -0.197\mathrm{b}_{1}-0.152\mathrm{b}_{3}+0.250\mathrm{b}_{48}\\
&\quad-0.197\mathrm{b}_{49}-0.152\mathrm{b}_{51}+0.250I,\\
\mathrm{P}(\mathrm{A}_0=-1,\,\mathrm{E}_0=+1) &= 0.197\mathrm{b}_{1}+0.152\mathrm{b}_{3}-0.250\mathrm{B}_{48}\\
&\quad-0.197\mathrm{b}_{49}-0.152\mathrm{b}_{51}+0.250I,\\
\mathrm{P}(\mathrm{A}_0=-1,\,\mathrm{E}_0=-1) &= -0.197\mathrm{b}_{1}-0.152\mathrm{b}_{3}-0.250\mathrm{b}_{48}\\
&\quad+0.197\mathrm{b}_{49}+0.152\mathrm{b}_{51}+0.250I,\\
\mathrm{P}(\mathrm{A}_0=+1,\,\mathrm{E}_1=+1) &= 0.074\mathrm{b}_{1}+0.238\mathrm{b}_{3}+0.250\mathrm{b}_{48}\\
&\quad+0.074\mathrm{b}_{49}+0.238\mathrm{b}_{51}+0.250I,\\
\mathrm{P}(\mathrm{A}_0=+1,\,\mathrm{E}_1=-1) &= -0.074\mathrm{b}_{1}-0.238\mathrm{b}_{3}+0.250\mathrm{b}_{48}\\
&\quad-0.074\mathrm{b}_{49}-0.238\mathrm{b}_{51}+0.250I,\\
\mathrm{P}(\mathrm{A}_0=-1,\,\mathrm{E}_1=+1) &= 0.074\mathrm{b}_{1}+0.238\mathrm{b}_{3}-0.250\mathrm{b}_{48}\\
&\quad-0.074\mathrm{b}_{49}-0.238\mathrm{b}_{51}+0.250I,\\
\mathrm{P}(\mathrm{A}_0=-1,\,\mathrm{E}_1=-1) &= -0.074\mathrm{b}_{1}-0.238\mathrm{b}_{3}-0.250\mathrm{b}_{48}\\
&\quad+0.074\mathrm{b}_{49}+0.238\mathrm{b}_{51}+0.250I,
\end{aligned}
\tag{A4}
$$

$$
\begin{aligned}
\mathrm{P}(\mathrm{E}_1=+1,\,\mathrm{A}_1=+1) &= 0.143\mathrm{b}_{1}+0.074\mathrm{b}_{16}+0.042\mathrm{b}_{17}\\
&\quad+0.061\mathrm{b}_{19}+0.205\mathrm{b}_{3}+0.238\mathrm{b}_{48}\\
&\quad+0.136\mathrm{b}_{49}+0.195\mathrm{B}_{51}+0.250I,\\
\mathrm{P}(\mathrm{E}_1=+1,\,\mathrm{A}_1=-1) &= -0.143\mathrm{b}_{1}+0.074\mathrm{b}_{16}-0.042\mathrm{b}_{17}\\
&\quad-0.061\mathrm{b}_{19}-0.205\mathrm{b}_{3}+0.238\mathrm{b}_{48}\\
&\quad-0.136\mathrm{b}_{49}-0.195\mathrm{b}_{51}+0.250I,\\
\mathrm{P}(\mathrm{E}_1=-1,\,\mathrm{A}_1=+1) &= 0.1430\mathrm{b}_{1}-0.074\mathrm{b}_{16}-0.042\mathrm{b}_{17}\\
&\quad-0.061\mathrm{b}_{19}+0.205\mathrm{b}_{3}-0.238\mathrm{b}_{48}\\
&\quad-0.136\mathrm{b}_{49}-0.195\mathrm{b}_{51}+0.250I,\\
\mathrm{P}(\mathrm{E}_1=-1,\,\mathrm{A}_1=-1) &= -0.143\mathrm{b}_{1}-0.074\mathrm{b}_{16}+0.042\mathrm{b}_{17}\\
&\quad+0.061\mathrm{b}_{19}-0.205\mathrm{b}_{3}-0.238\mathrm{b}_{48}\\
&\quad+0.136\mathrm{b}_{49}+0.195\mathrm{b}_{51}+0.250I,
\end{aligned}
\tag{A5}
$$

$$
\begin{aligned}
\mathrm{P}(\mathrm{A}_1=+1,\,\mathrm{E}_0=+1) &= 0.197\mathrm{b}_{1}+0.143\mathrm{b}_{16}+0.113\mathrm{b}_{17}\\
&\quad+0.078\mathrm{b}_{19}+0.152\mathrm{b}_{3}+0.205\mathrm{b}_{48}\\
&\quad+0.162\mathrm{b}_{49}+0.125\mathrm{b}_{51}+0.250I,\\
\mathrm{P}(\mathrm{A}_1=+1,\,\mathrm{E}_0=-1) &= -0.197\mathrm{b}_{1}+0.143\mathrm{b}_{16}-0.113\mathrm{b}_{17}\\
&\quad-0.078\mathrm{b}_{19}-0.152\mathrm{b}_{3}+0.205\mathrm{b}_{48}\\
&\quad-0.162\mathrm{b}_{49}-0.125\mathrm{b}_{51}+0.250I,\\
\mathrm{P}(\mathrm{A}_1=-1,\,\mathrm{E}_0=+1) &= 0.197\mathrm{b}_{1}-0.143\mathrm{b}_{16}-0.113\mathrm{b}_{17}\\
&\quad-0.078\mathrm{b}_{19}+0.152\mathrm{b}_{3}-0.205\mathrm{b}_{48}\\
&\quad-0.162\mathrm{b}_{49}-0.125\mathrm{b}_{51}+0.250I,\\
\mathrm{P}(\mathrm{A}_1=-1,\,\mathrm{E}_0=-1) &= -0.197\mathrm{b}_{1}-0.143\mathrm{b}_{16}+0.113\mathrm{b}_{17}\\
&\quad+0.078\mathrm{b}_{19}-0.152\mathrm{b}_{3}-0.205\mathrm{b}_{48}\\
&\quad+0.162\mathrm{b}_{49}+0.125\mathrm{b}_{51}+0.250I.
\end{aligned}
\tag{A6}
$$

where $\mathrm{b}_i = \mathrm{tr}(\rho \mathrm{B}_i)$ with B_i are the Pauli operators. The order of B_i is in the four-base subscript and the base-four notation, 0, 1, 2, 3 can be directly mapped to either identity or Pauli x, y, and z matrices. For example B_3 has the form $I \otimes I \otimes \sigma_z$ where I, σ_z are identity and Pauli z matrices, respectively. Similarly we can find the forms of other B_i (details are given in [49]).

[1] N. Brunner, D. Cavalcanti, S. Pironio, V. Scarani, and S. Wehner, Rev. Mod. Phys. **86**, 419 (2014).

[2] J. F. Clauser, M. A. Horne, A. Shimony, and R. A. Holt, Phys. Rev. Lett. **23**, 880 (1969).

[3] J. S. BELL, Rev. Mod. Phys. **38**, 447 (1966).

[4] D. Collins, N. Gisin, N. Linden, S. Massar, and S. Popescu, Phys. Rev. Lett. **88**, 040404 (2002).

[5] S. Kochen and E. P. Specker, "The problem of hidden variables in quantum mechanics," in *The Logico-Algebraic Approach to Quantum Mechanics: Volume I: Historical Evolution*, edited by C. A. Hooker (Springer Netherlands, Dordrecht, 1975) pp. 293–328.

[6] A. Acín, T. Fritz, A. Leverrier, and A. B. Sainz, Communications in Mathematical Physics **334**, 533 (2015).

[7] M. Araújo, M. T. Quintino, C. Budroni, M. T. Cunha, and A. Cabello, Phys. Rev. A **88**, 022118 (2013).

[8] B. Amaral, M. T. Cunha, and A. Cabello, Phys. Rev. A **89**, 030101 (2014).

[9] A. Cabello, S. Severini, and A. Winter, Phys. Rev. Lett. **112**, 040401 (2014).

[10] J.-A. Larsson, M. Giustina, J. Kofler, B. Wittmann, R. Ursin, and S. Ramelow, Phys. Rev. A **90**, 032107 (2014).

[11] M. Giustina, M. A. M. Versteegh, S. Wengerowsky, J. Handsteiner, A. Hochrainer, K. Phelan, F. Steinlechner, J. Kofler, J.-A. Larsson, C. Abellán, W. Amaya,

V. Pruneri, M. W. Mitchell, J. Beyer, T. Gerrits, A. E. Lita, L. K. Shalm, S. W. Nam, T. Scheidl, R. Ursin, B. Wittmann, and A. Zeilinger, Phys. Rev. Lett. **115**, 250401 (2015).
[12] L. K. Shalm, E. Meyer-Scott, B. G. Christensen, P. Bierhorst, M. A. Wayne, M. J. Stevens, T. Gerrits, S. Glancy, D. R. Hamel, M. S. Allman, K. J. Coakley, S. D. Dyer, C. Hodge, A. E. Lita, V. B. Verma, C. Lambrocco, E. Tortorici, A. L. Migdall, Y. Zhang, D. R. Kumor, W. H. Farr, F. Marsili, M. D. Shaw, J. A. Stern, C. Abellán, W. Amaya, V. Pruneri, T. Jennewein, M. W. Mitchell, P. G. Kwiat, J. C. Bienfang, R. P. Mirin, E. Knill, and S. W. Nam, Phys. Rev. Lett. **115**, 250402 (2015).
[13] S. Dogra, K. Dorai, and Arvind, Physics Letters A **380**, 1941 (2016).
[14] G. Kirchmair, F. Zähringer, R. Gerritsma, M. Kleinmann, O. Gühne, A. Cabello, R. Blatt, and C. F. Roos, Nature **460**, 494 EP (2009).
[15] A. A. Klyachko, M. A. Can, S. Binicioğlu, and A. S. Shumovsky, Phys. Rev. Lett. **101**, 020403 (2008).
[16] S. Popescu and D. Rohrlich, Physics Letters A **169**, 411 (1992).
[17] S. L. Braunstein, A. Mann, and M. Revzen, Phys. Rev. Lett. **68**, 3259 (1992).
[18] E. Diamanti, H.-K. Lo, B. Qi, and Z. Yuan, Npj Quantum Information **2**, 16025 EP (2016).
[19] V. Scarani, H. Bechmann-Pasquinucci, N. J. Cerf, M. Dušek, N. Lütkenhaus, and M. Peev, Rev. Mod. Phys. **81**, 1301 (2009).
[20] A. Acín, N. Gisin, and L. Masanes, Phys. Rev. Lett. **97**, 120405 (2006).
[21] U. Vazirani and T. Vidick, Phys. Rev. Lett. **113**, 140501 (2014).
[22] A. Acín and L. Masanes, Nature **540**, 213 EP (2016).
[23] A. Acín, N. Gisin, and L. Masanes, Phys. Rev. Lett. **97**, 120405 (2006).
[24] M. Pawłowski, Phys. Rev. A **82**, 032313 (2010).
[25] D. Saha and R. Ramanathan, Phys. Rev. A **95**, 030104 (2017).
[26] T. Li, X. Zhang, Q. Zeng, B. Wang, and X. Zhang, Opt. Express **26**, 11959 (2018).
[27] M. Pawłowski and i. c. v. Brukner, Phys. Rev. Lett. **102**, 030403 (2009).
[28] R. Ramanathan, A. Soeda, P. Kurzyński, and D. Kaszlikowski, Phys. Rev. Lett. **109**, 050404 (2012).
[29] P. Kurzyński, A. Cabello, and D. Kaszlikowski, Phys. Rev. Lett. **112**, 100401 (2014).
[30] X. Zhan, X. Zhang, J. Li, Y. Zhang, B. C. Sanders, and P. Xue, Phys. Rev. Lett. **116**, 090401 (2016).
[31] S. L. Braunstein and C. M. Caves, Phys. Rev. Lett. **61**, 662 (1988).
[32] R. Chaves and C. Budroni, Phys. Rev. Lett. **116**, 240501 (2016).
[33] R. Chaves, Phys. Rev. A **87**, 022102 (2013).
[34] R. Chaves and T. Fritz, Phys. Rev. A **85**, 032113 (2012).
[35] L.-Z. Cao, J.-Q. Zhao, X. Liu, Y. Yang, Y.-D. Li, X.-Q. Wang, Z.-B. Chen, and H.-X. Lu, Scientific Reports **6**, 23758 EP (2016).
[36] H. Katiyar, A. Shukla, K. R. K. Rao, and T. S. Mahesh, Phys. Rev. A **87**, 052102 (2013).
[37] L.-Z. Cao, J.-Q. Zhao, X. Liu, Y. Yang, Y.-D. Li, X.-Q. Wang, Z.-B. Chen, and H.-X. Lu, Scientific Reports **6**, 23758 (2016).
[38] X. Zhan, P. Kurzyński, D. Kaszlikowski, K. Wang, Z. Bian, Y. Zhang, and P. Xue, Phys. Rev. Lett. **119**, 220403 (2017).
[39] D. Qu, P. Kurzyński, D. Kaszlikowski, S. Raeisi, L. Xiao, K. Wang, X. Zhan, and P. Xue, Phys. Rev. A **101**, 060101 (2020).
[40] P. Kurzyński and D. Kaszlikowski, Phys. Rev. A **89**, 012103 (2014).
[41] A. Cabello, S. Severini, and A. Winter, Phys. Rev. Lett. **112**, 040401 (2014).
[42] P. Kurzyński, R. Ramanathan, and D. Kaszlikowski, Phys. Rev. Lett. **109**, 020404 (2012).
[43] A. Mitra, K. Sivapriya, and A. Kumar, J. Magn. Reson. **187**, 306—313 (2007).
[44] A. Gaikwad, Arvind, and K. Dorai, Quantum Information Processing **20**, 19 (2021).
[45] I. S. Oliveira, T. J. Bonagamba, R. S. Sarthour, J. C. C. Freitas, and E. R. deAzevedo, *NMR Quantum Information Processing* (Elsevier, Linacre House, Jordan Hill, Oxford OX2 8DP, UK, 2007).
[46] E. Knill, I. Chuang, and R. Laflamme, Phys. Rev. A **57**, 3348 (1998).
[47] A. Singh, A. Gautam, Arvind, and K. Dorai, Physics Letters A **383**, 1549 (2019).
[48] D. Singh, J. Singh, K. Dorai, and Arvind, Phys. Rev. A **100**, 022109 (2019).
[49] A. Singh, H. Singh, K. Dorai, and Arvind, Phys. Rev. A **98**, 032301 (2018).